Nanoliposomal Omega-3 Fatty Acids Promote Adult Hippocampal Neurogenesis through the BDNF/TrkB Pathway in C57BL/6 Mice

Foltran RB*[1], Diaz G*[2,3,4], Stefani KM[5,6], Feliu MS[7], Impa Condori AR[7], Colapietro AA[5,6], Montagna DR[8,9], Ambrosi V[2,3,4,10], Godoy MF[7], Guidi SM[2,3,10], Nanni M[11], Diaz SL[8,12]

*These authors contributed equally to this article

[1] Instituto de Fisiología, Biología Molecular y Neurociencias (IFIBYNE), UBA-CONICET, Buenos Aires, Argentina.

[2] Instituto Tecnología de Alimentos, INTA, Buenos Aires, Argentina.

[3] Instituto de Ciencia y Tecnología de Sistemas Alimentarios Sustentables (ICyTeSAS) INTA – CONICET, Buenos Aires, Argentina.

[4] Facultad de Farmacia y Bioquímica (FFyB), Cátedra de Bromatología, UBA. Buenos Aires, Argentina.

[5] Instituto de Biología Celular y Neurociencias (IBCN), UBA-CONICET, Buenos Aires, Argentina.

[6] Universidad Argentina de la Empresa (UADE). Buenos Aires, Argentina.

[7] Facultad de Farmacia y Bioquímica (FFyB), Cátedra de Nutrición, UBA. Buenos Aires, Argentina.

[8] Instituto de Biociencias, Biotecnología y Biología traslacional (IB3), UBA-CONICET. Buenos Aires, Argentina.

[9] Facultad de Ciencias Veterinarias (FVET), Cátedra de Química Biológica, UBA. Buenos Aires, Argetina.

[10] Universidad de Moron, Escuela Superior de Ingeniería, Informática y Ciencias Agroalimentarias (ESIICA, UM), Argentina.

[11] Universidad Nacional de Hurlingham (UNAHUR), Argentina.

[12] Facultad de Farmacia y Bioquímica (FFyB), Cátedra de Técnicas de Bioterio, UBA. Buenos Aires, Argentina.

Abstract

Polyunsaturated fatty acids (PUFAs) are fundamental for different cellular and structural processes, especially regarding the nervous system. However, its incorporation in food has many bioaccessibility limitations, making it important to find new ways of its consumption. In this work, nanoencapsulated PUFAs orally administrated to C57BL/6 elite male mice for 8 weeks showed better bioavailability when compared to administration of free acids, also improving the effects on dentate gyrus neuronal survival as well as on the proneurogenic elements of the Brain derived neurotrophic factor biological pathway also in the hippocampus. In addition, nanoencapsulated PUFAs increased expression of Fabp5, a relevant n-3 fatty acids transporter in the brain. Altogether, our results would mean that the form of administration of the fatty acids can alter not only how much and how preserved they reach the central nervous system, but also have a differential impact in the diverse processes they contribute to.

Introduction

Polyunsaturated fatty acids (PUFAs) are indispensable structural and signaling components of cellular architecture. Scientific interest in neurobiology focuses on omega-3 Polyunsaturated fatty acids (*n*-3 PUFAs), specifically, eicosapentaenoic acid (20:5, *n*-3; EPA) and docosahexaenoic acid (22:6, *n*-3; DHA). These molecules are far more than energy substrates: they are preferentially esterified into neuronal membrane phospholipids. Within this lipid bilayer, their high degree of unsaturation modulates critical physicochemical properties, i.e. membrane fluidity, curvature, and the spatial organization of lipid rafts, essential for neurotransmission and synaptic plasticity (1,2).

The physiological efficacy of n-3 PUFAs is dictated by their transition from the diet to the brain parenchyma, a process restricted by the blood-brain barrier (BBB). Recent evidence identifies the Major Facilitator Superfamily Domain-containing protein 2a (MFSD2A) as the primary transporter for lysophosphatidylcholine-bound DHA, while the Fatty Acid-Binding Protein 5

53 (*Fabp5*) facilitates the uptake of non-esterified forms (3,4). Collectively, this coordinated
54 transport mechanism represents the physiological bottleneck that determines the
55 neuroprotective efficacy of lipids.

56 Furthermore, the modern "Western Diet" has shifted the systemic lipid profile toward a pro-
57 inflammatory state, characterized by an excessive *n*-6/*n*-3 ratio and high Saturated Fatty-Acids
58 (SFA) intake, which respectively competes with *n*-3 PUFAs for desaturation and elongation
59 pathways, and promote membrane lipid remodeling that limits n-3 PUFA incorporation (5).
60 Conventional n-3 incorporation in food, however, is hindered by the extreme susceptibility of
61 methylene-interrupted double bonds to oxidative stress. The resulting lipid peroxidation
62 products not only diminish biological functionality but can also induce cellular toxicity.

63 To overcome these bioaccessibility limitations, the use of fermented dairy matrices offers a
64 promising strategy as a carrier for omega-3 fatty acids, owing to their ability to optimize
65 bioactive stability and functionality. Furthermore, nanotechnology-specifically through
66 nanoemulsions and encapsulation-has been established as a superior strategy to enhance lipid
67 delivery (6). By protecting PUFAs from gastric degradation and optimizing intestinal
68 micellization, these systems significantly increase the concentration of active fatty acids in target
69 tissues (7).

70 A central objective of this research is to elucidate how this enhanced omega-3 fatty acids
71 delivery impacts adult hippocampal neurogenesis in a murine model. The dentate gyrus (DG)
72 maintains a neurogenic niche where multipotent stem cells expressing Nestin (Nes) transition
73 into mature, Calbindin-positive (Calb1) functional neurons (8). This continuum is orchestrated
74 by the Brain-Derived Neurotrophic Factor (BDNF) pathway, among other factors. The BDNF is
75 synthesized as a pro-protein, the 32 kDa pro-BDNF that may be cleaved to yield the 13.2-15.9
76 kDa mature BDNF (mBDNF). The pro-BDNF can release mBDNF after cleavage either intra- or
77 extra-cellularly, or be secreted as pro-BDNF without further modifications. By binding to TrkB
78 receptors, the mBDNF facilitates pro-neurogenic effects, whereas the pro-BDNF may bind

79 different receptors, being the most known the p75, through which pro-apoptotic actions are
80 promoted (see a rev. in (9)). While DHA is known to upregulate BDNF (10,11), the specific
81 molecular mechanisms by which nanoencapsulated n-3 PUFAs (DHA-EPA) modulate the
82 expression of markers of neuronal differentiation during this process remain under-investigated.
83 Therefore, the present study evaluates the effects of orally administered nanoencapsulated n-3
84 PUFAs (DHA-EPA), delivered via a fermented yogurt matrix, in male C57BL/6 mice over a chronic
85 period. The administration of the bioactive compounds was based on the Recommended Daily
86 Intake (RDI) of at least 250mg/day of EPA+DHA for healthy adults (excluding non-pregnant/non-
87 lactating adult females) established by international organizations (12), integrated into a
88 fermented dairy matrix to ensure its bioavailability and mimic an optimized human consumption
89 scenario. We hypothesize that this formulation increases systemic bioavailability, BBB transport
90 efficiency, and metabolic incorporation compared to free fatty acids, thereby enhancing
91 neuronal survival in the DG and robustly activating the BDNF signaling cascade.
92

Materials and Methods

Animals

Studies were performed on 51 male, C57BL/6 elite mice purchased at the Instituto de Medicina Experimental, Academia Nacional de Medicina, Buenos Aires, Argentina. Experiments on animals were conducted according to local regulations and were approved by the Institutional Ethical Committee (ResCD-2022-1246-E-UBA-DCT#FMED). Three-four-week-old mice, bred in barrier-conditions to maintain an SPF status, were transported in environmentally controlled conditions to our institute's animal facility. After arrival, mice were housed in 1284L Eurostandard Type II Long (365 mm × 207 mm × 140 mm) Tecniplast microisolator cages with filter tops (five to six animals per cage), with autoclavated aspen shavings as bedding and tissue paper as nesting material. Mice were maintained under controlled conditions, i.e., 22 ± 2°C room temperature, 40-70% relative humidity, 12–12 h light–dark cycle (lights on at 8 a.m.), pelleted food for rodents (Cooperación) and water ad libitum. Cages were changed twice a week. A period of acclimation of 2 weeks was left before the beginning of experiments, and therefore, mice were 5–6 week-old when treatments began.

Yogurt preparation and administration

Raw Materials and Starter Culture

Yogurt was manufactured using commercial pasteurized cow milk (2% w/v fat; *Mastellone Hnos. S.A., Buenos Aires, Argentina*). A lyophilized Direct Vat Set (DVS) thermophilic starter culture, YoFlex® YG-X16 (comprising *Streptococcus thermophilus* and *Lactobacillus delbrueckii* subsp. *bulgaricus*), was provided by Chr. Hansen (Hørsholm, Denmark). Prior to inoculation, the culture was activated by hydrating 3 g of the lyophilized powder in 1000 mL of milk at 45 °C according to the manufacturer's instructions.

119 *Functional Ingredients and Yogurt Preparation*

120 Omega-3 oil (MEG-3™ 2050EE) was sourced from DSM Nutritional Products. Three distinct
121 formulations were established based on the omega-3 delivery system:

122 • Control: Yogurt without oil supplementation.

123 • Free Acids: Yogurt supplemented with bulk omega-3 oil (250 mg / 200 mL milk).

124 • Nano Acids: Yogurt supplemented with a nanoencapsulated omega-3/soy lecithin
125 formulation. To achieve an equivalent dose of 250 mg of active omega-3 per 200 mL (provided
126 by Nanotica Agro SRL via an R&D agreement with INTA) was incorporated.

127 In both functional formulations, bioactive compounds were homogenized into the milk-sugar
128 base (75 g/L) prior to fermentation.

129 *Yogurt Manufacturing*

130 The mixtures were inoculated with the activated starter culture (2 mL/L) and aseptically
131 distributed into 200 g sterile polypropylene containers. Incubation was performed at 43 ± 1 °C
132 until a target pH of 4.5 was achieved. Samples were then cooled and stored at 4 °C for 28 days
133 for analysis.

134 *Yogurt Administration*

135 The different formulations of yogurt were administered to mice by mixing it with a palatable
136 cube. They were made with 10 g of powdered yeast, 66 g of powdered milk, 36 g of sugar, and
137 14 g of gelatin, for each ice tray (12 cubes) (13). These ingredients were mixed with 2 ml of each
138 of the three yogurts and with approximately 60 mL of tap water, forming a thick liquid
139 preparation, which was poured into an ice tray. The 3 cm × 3 cm × 4 cm cubes, weighing around
140 12 g, were kept at 4 °C and were prepared every 6 days. A yogurt containing cube was given per
141 cage, every day between 2 p.m. and 5 p.m. Mice voluntarily ate the cubes, immediately after
142 they were placed in the cages.

143

144

145 **Experiments:**

146 All mice were divided into 3 groups (control vs the two types of yogurt formulation) for 3
147 different experiments. For the first protocol, 5 mice per group were administered the yogurt
148 cubes for 4 weeks. At the end of the treatment, all mice were deeply anesthetized (20 mg/kg
149 xylazine and 200 mg/kg ketamine) and blood was obtained by intracardiac collection, from
150 which serum was extracted to quantify fatty acids concentrations. After death confirmation,
151 mice were decapitated, brains were removed, and both hippocampus (HC) were obtained,
152 where the left hemi-HCs were prepared for protein extraction and Western blots and the right
153 hemi-HCs were used for mRNA measurements by qRT-PCR.

154 For the second experiment, in order to study neuronal proliferation 18 mice (n = 6 per group)
155 were administered yogurt cubes for 4 weeks. The thymidine analog 5-bromo-2'-deoxyuridine
156 (BrdU; Sigma, B9285) was administered to mice at the end of the treatment, in order to label
157 dividing cells. Animals received two ip injections of BrdU, 50 mg/kg each, at a 2 h interval. BrdU
158 was dissolved in 0.9% NaCl at 50 °C. The next day, all mice were deeply anesthetized (20 mg/kg
159 xylazine and 200 mg/kg ketamine) and transcardially perfused with 5 mL of 0.9% NaCl with
160 heparin and 50 mL of 4% paraformaldehyde in 0.1 M phosphate-buffered saline (PBS, pH 7.4)
161 for 15 min. Brains were recovered, post-fixed for 24 h at 4 °C, and cryoprotected with a 30%
162 sucrose solution. Brains were then sliced into 35 µm thick coronal sections through the
163 hippocampus (bregma −0.94 to −3.80) with a freezing microtome. Sections were stored at 4 °C
164 in 0.1 M PBS with 0.1% sodium azide if not used immediately.

165 For the last trial, the yogurt cubes were administered for 8 weeks to 18 mice (6 per group) to
166 study the survival of newborn neurons. Animals received two ip injections of BrdU, 50 mg/kg
167 each, at a 2 h interval for two consecutive days at the end of the 4th week of treatment. Mice
168 were then continued treatment for 4 more weeks, so that BrdU labeled 4 week-old neurons. At
169 the end of the treatment, all mice were deeply anesthetized and transcardially perfused, as
170 stated before.

171

172 **Fatty acid profile determination**

173 Serum fatty acid profile was determined by gas chromatography: Chromatograph: Perkin Elmer
174 Clarus 500; Column: Supelco SP 2560 100 m x 0.25 mm x 0.20 µm; FID detector 280 °C; Carrier
175 gas: helium. Previously, serum lipids were converted into methyl esters according to the Lepage
176 and Roy method as follows: 2 mL of methanol/toluene (4:1) were added to 200 µL of serum,
177 followed by 0.2 mL of acetyl chloride using a vortex mixer. The mixture was incubated at 100 °C
178 for one hour. Then, 5 mL of 6% potassium carbonate was added, and the samples were
179 centrifuged; 1 µL of the toluene layer was injected into the chromatograph. Fatty acid methyl
180 esters (FAMEs) were identified based on their retention times by comparison with the PUFA No.
181 2 (Animal Source) FAME analytical standard (SUPELCO 47015-U). The results (mean ±SD) were
182 expressed as the per cent (%) of total fatty acids content, with a quantification limit of 0.05%
183 (14).

184

185 **Western Blotting**

186 Tissue was homogenized with 250 µl of RIPA buffer (150 mM NaCl, 1% NP-40, 0.5% Sodium
187 deoxycholate, 0.1% SDS, 50 mM Tris) along with protease inhibitors (1:100) and centrifuged at
188 4°C for 30 min at 13000 (r/min). The supernatants were recovered and protein levels were
189 quantified by the Bradford protein assay. Samples (50 µgr in 5× loading buffer) were then loaded
190 into SDS-PAGE gels (12 or 15%) and transferred onto nitrocellulose membranes using the Mini-
191 PROTEAN® Tetra System (BIO-RAD) for 1 h.

192 Membranes were incubated for 1 h with blocking solution (5% milk in TBST) and then probed
193 overnight at 4°C with mouse anti-BDNF (1:2000; Icosagen; 327-100 clone 3C11), rabbit anti-p75
194 (1:700; Alomone Labs; ANT-007), rabbit anti-TrkB (1:700; Alomone Labs; ANT-019), and rabbit
195 anti-proBDNF (1:2500; Genocopoeia) in TBST. Actin was used as a loading control (1:2000; Santa
196 Cruz). Binding of primary antibodies was visualized with anti-mouse HRP-conjugated secondary

197 antibody (1:20000; Invitrogen) or anti-rabbit HRP-conjugated secondary antibody (1:20000;
198 Invitrogen). Membranes were developed using the ECL Plus Western blotting substrate (Thermo
199 Fisher Scientific) for chemiluminescence with the Gene Gnome® Imager. Densitometry was
200 carried out using ImageJ software (15). The signal of each protein is expressed after subtraction
201 of background signal and related to actin signal.
202
203 **qRT-PCR**
204 Hippocampal tissue was collected in 250 µL cold Trizol (Invitrogen, Paisley, UK) and
205 homogenized using plastic pestles for homogenizers. RNA was isolated according to the
206 manufacturer's protocol. After addition of chloroform, samples were centrifuged at 11,000 × g
207 for 15 min at 4 °C. The aqueous phase was transferred and RNA was precipitated with
208 isopropanol, washed with 75% ethanol and resuspended in 15 µL of RNase-free DEPC-treated
209 water. RNA concentration of the tissue was quantified with the Qubit 2.0 Fluorometer (RNA
210 Assay BR Kit, Invitrogen). To ensure genomic DNA removal, 1 µg of total RNA was treated with
211 1 U/µL of DNase I (Invitrogen) for 15 min. RNA purity and absence of residual DNA were verified
212 by qPCR using non-reverse-transcribed RNA as a negative control. Samples were stored at −80
213 °C until further use.
214 Reverse Transcription Quantitative Polymerase Chain Reaction (qRT-PCR) was carried out in a
215 StepOnePlus Real-Time PCR System (Applied Biosystems, CA, USA), and the data were analyzed
216 with StepOne software v2.2. The retrotranscription and amplification reactions were performed
217 in a total volume of 10 µl buffer solution containing 2 µl of template RNA, 5 µl of 2× iTaq universal
218 SYBR® Green reaction mix (2x), 0.125 µl iScript reverse transcriptase (Applied Biosystems), 2.08
219 µl RNase-free DEPC-treated water and 0.4 µl of each primer (400 µM). Primers for BDNF (Brain-
220 Derived Neurotrophic Factor), FABP5 (Fatty Acid Binding Protein 5), Calb1 (Calbindin) and Nes
221 (Nestin) were designed using Primer Express software (Applied Biosystems) and described in
222 table 1.

The thermal cycling profile consisted of:

-UNG pre-incubation: 50 °C for 2 min.

-Initial denaturation: 95 °C for 1 min.

-Amplification (40 cycles): 95 °C for 15 s and 60 °C for 1 min.

-Melt curve analysis: 95 °C (15 s), 60 °C (1 min), and a final ramp to 95 °C at 0.6 °C/s to confirm amplicon specificity.

To ensure the robustness of the gene expression analysis, three independent biological replicates were processed per experimental group, following the recommendations of the MIQE guidelines (16). Each biological sample was analyzed in triplicate using qRT-PCR. This balanced design allows for an accurate estimation of experimental error even with biological sample sizes of n=3, ensuring that the observed differences possess true statistical and biological significance. Target gene expression was normalized against β-actin (ACTB) as the internal reference gene. The dynamic range was established using a six-point standard curve derived from three independent biological replicates, each processed in technical triplicate (n=9 per dilution). R^2 values and amplification efficiencies were calculated based on mean Cq values, incorporating a housekeeping gene (also analyzed in triplicate) for normalization. CT (threshold cycle) values were calculated by subtracting the CT value of ACTB from the CT values. Relative expression was calculated as E^−ΔCt, where E is the efficiency measured for each set of primers.

Gene Symbol	**Accession No.**	**Primer Sequence (5' →3')**	***E* (%)**	**R^2**	**Dynamic Range**
Actb	NM_007393.5	**F:** ACCAGTTCGCCATGGATGAC **R:** TGCCGGAGCCGTTGTC	97.019	0.995	10^2 - 10^7
Bdnf	NM_001285418.1	**F:** CATAGACAAAAGGCACTGGAACTC **R:** TAAGGGCCCGAACATACGAT	92.000	0.980	10^2 - 10^7
Fabp5	BC002008.1	**F:** CGACAGCTGATGGCAGAAAA **R:** CAGGCCACCGTCTTGGAA	91.788	0.993	10^2 - 10^7

Calb1	NM_009788.4	**F:** GCTCCGCGCACTCTCAA **R:** TGACTGCAGGTGGGATTCTG	98.828	0.940	10^2 - 10^7
Nes	NM_016701.3	**F:** GGTCACTGTCGCCGCTACTC **R:** AAGCGGACGTGGAGCACTA	94.788	0.989	10^2 - 10^7

Table 1. Primer sequences and qPCR performance characteristics. Accession No. refers to the NCBI GenBank database. $\boldsymbol{E}$ **(%)** represents the amplification efficiency calculated from the slope of the standard curve (E=[$10^{(-1/slope)}$–1]×100. $\boldsymbol{R}^2$ denotes the coefficient of determination for the linear regression. **Dynamic Range** indicates the interval of template concentration where linearity was maintained. All assays were performed in technical triplicate using SYBR Green chemistry on a StepOnePlus™ Real-Time PCR System.

Immunofluorescence

Newborn cells in the dentate gyrus (DG) were revealed by immunostaining against BrdU as previously published (17). Free-floating sections were exposed to 2 N HCl for 1 h. Nonspecific binding was reduced by 1 h incubation in a saturation solution containing 2 g/L gelatin (Merck) and 0.25% triton in PBS. Sections were then incubated overnight at 4 °C with a mouse anti-BrdU antibody (1:1000; Developmental Studies Hybridoma Bank, concentrated). Next day, the tissue was incubated for 2 h with an anti-mouse-A488 (1: 500; Invitrogen). All primary and secondary antibodies were diluted in the saturation solution. Finally, sections were incubated with Hoechst (1: 10000, Invitrogen) to dye the nucleus of cells. The number of BrdU-labeled cells was quantified with a fluorescence microscope (Olympus IX81) with a 20× objective, on serial sections through the entire hippocampus. One out of six series was counted (180 µm intervals, 10 sections per series). BrdU-labeled cells were counted in the sub-granular zone of the granule-cell layer over the entire DG. Cells were considered to be $BrdU^+$ when their nuclei were completely filled with fluorescence or showed clear patches of variable intensity (classic dilution pattern for survival assays).

Statistical Analysis

Group differences were analyzed using one-way analysis of variance (ANOVA). Assumptions of normality and homogeneity of variances were assessed using the Shapiro–Wilk and Bartlett tests, respectively. When variance heterogeneity was detected, statistical analyses were performed using either Welch's one-way ANOVA or generalized least squares (GLS) models that explicitly accounted for heteroscedasticity. For GLS analyses, models allowing different variance structures were compared to homoscedastic models using likelihood ratio tests, and the final model was selected by balancing goodness-of-fit and parsimony. Post hoc comparisons were performed using Tukey's test following classical ANOVA and GLS models, whereas Games–Howell tests were used following Welch's ANOVA. In fatty acid analyses, p-values were adjusted for multiple testing using the Benjamini–Hochberg false discovery rate (FDR) procedure, applied separately to individual fatty acids and fatty acid classes. Body weight was analyzed using a two-way repeated-measures ANOVA with week as a within-subject factor and treatment as a between-subject factor. Sphericity was assessed using Mauchly's test and Geenhouse-Geisser corrections were applied when necessary. In all analyses, $p < 0.05$ was considered statistically significant, whereas values between 0.05 and 0.1 were considered a trend.

282 **Results**

283 *Body weight*

284 Mice were weighed across every week of treatment to control for potential changes due to the
285 different treatments. Analyses showed an interaction between treatment and number of weeks
286 ($p = 0.030$), with no difference in treatment ($p = 0.145$) but significant changes across weeks (p
287 $<.001$). As expected, given their age, all mice gained some weight along the experimental
288 protocol but no differences were revealed between experimental groups.

289

290 *Fatty acids profile*

291 Individual serum levels of the SFA lauric (C12:0), myristic (C14:0) and palmitic (C16:0) were not
292 altered by the treatments ($p = 0.2482$, $p = 0.5138$, $p = 0.5962$), whereas the SFA stearic (C18:0)
293 and lignoceric (C24:0) showed a trend to higher values in the group that consumed the
294 nanoencapsulated version of omega-3 fatty acids in yogurt compared to the control group ($p =$
295 0.0697) (Table 2).

296 Both omega-3–fortified yogurt groups exhibited a trend to lower serum oleic acid (C18:1 n-9)
297 levels compared with the control group ($p = 0.0697$), whereas no effect was observed on
298 palmitoleic acid (C16:1 n-7) concentrations ($p = 0.5962$) (Table 2).

299 Regarding the essential PUFAs linoleic acid (C18:2 n-6) and α-linolenic acid (C18:3 n-3), no
300 significant differences were observed among groups ($p = 0.7495$, $p = 0.5138$). Likewise,
301 arachidonic acid (C20:4 n-6) levels were not significantly affected by the treatments ($p = 0.5138$)
302 (Table 2).

303 Eicosapentaenoic acid (EPA, C20:5 n-3) showed a trend toward higher serum concentrations in
304 the supplemented groups compared with the control (ANOVA $p = 0.07$; FDR-adjusted $p = 0.1633$)
305 (Figure 1.A; Table 2). The control group exhibited intra-group variability, whereas both omega-
306 3-enriched yogurt formulations resulted in more homogeneous and consistently elevated EPA
307 levels. Although these differences did not reach statistical significance after multiple-

308 comparison correction, the observed pattern suggests a potential treatment-related effect on

309 circulating EPA.

310 Docosahexaenoic acid DHA (C22:6 n-3) levels showed no significant differences in the free acids

311 group compared to the control group (p = 0.1973) (Figure 1.B). However, the nanoencapsulated

312 yogurt formulation produced a significant increase in serum DHA levels compared with both

313 control and free-fatty acids groups (p = 0,00007). As expected, the group consuming the

314 nanoencapsulated omega-3 yogurt exhibited a higher total n-3 fatty acid content (Figure 1.C)

315 and a lower n-6/n-3 ratio (Figure 1.D), relative to the other groups. This finding suggests that

316 nanoencapsulation may protect DHA from degradation during storage and digestion, thereby

317 enhancing its stability and facilitating intestinal absorption, as reflected by increased serum DHA

318 levels.

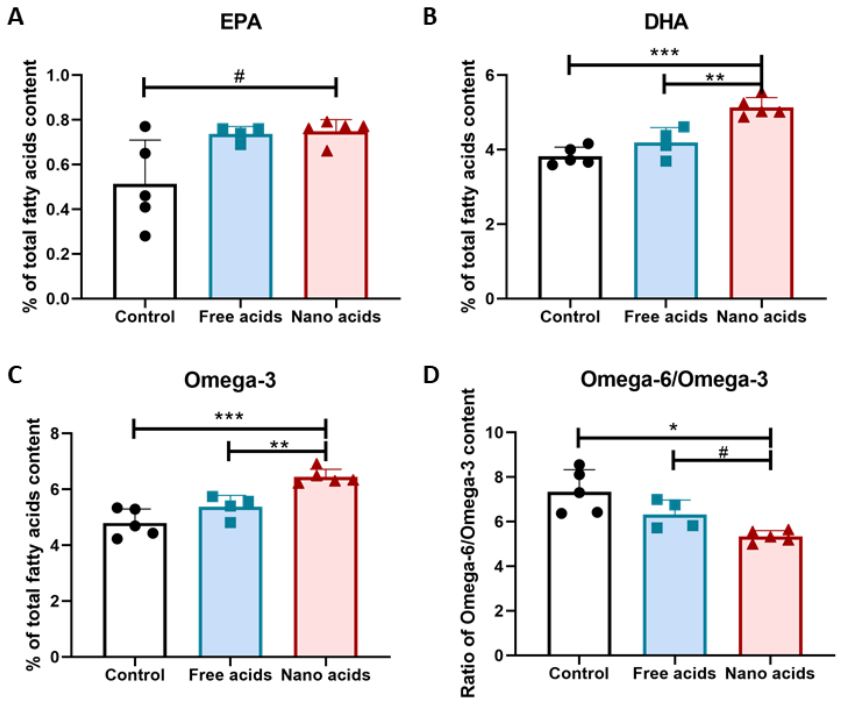

319

320 **Figure 1.** Omega-3 fatty acids profile and n-6/n-3 ratio in serum. Results are expressed as the

321 percentage (%) of total fatty acids content. (A-B) Individual % for DHA and EPA. (C) Total % of

322 fatty acids from the Omega-3 family. (D) Ratio of Omega-6/Omega-3 content in serum. Data are

323 expressed as mean ± SD, n =4-5/group. # 0.05 < p < 0.10; *p < 0.05; **p < 0.01; ***p < 0.001

324

Serum composition	Control	Free fatty acids	Nano fatty acids	Statistics	P value (FDR)
Lauric acid	0.07 ± 0.023	0.072 ± 0.026	0.052 ± 0.004	F_2 = 2.538	0.2482
Myristic acid	0.316 ± 0.056	0.355 ± 0.066	0.304 ± 0.036	F_2 = 1.1	0.5138
Palmitic acid	18.2 ± 0.765	19.2 ± 1.39	19 ± 1.72	F_2 = 0.713	0.5962
Stearic acid	8.48 ± 0.287	9.61 ± 0.972	9.46 ± 0.446*	F_2 = 9.025	0.0697
Lignoceric acid	0.166 ± 0.044	0.205 ± 0.031	0.284 ± 0.078*	F_2 = 5.692	0.0697
Oleic acid	17.3 ± 1.01	14.7 ± 1.94#	14.6 ± 1.39*	F_2 = 5.262	0.0697
Palmitoleic acid	3.71 ± 0.430	3.66 ± 0.512	3.37 ± 0.414	F_2 = 0.786	0.5962
Linoleic acid	20.9 ± 1.23	21.6 ± 1.97	21.5 ± 0.632	F_2 = 0.374	0.7495
Alfa-linolenic acid	0.622 ± 0.108	0.598 ± 0.045	0.684 ± 0.084	F_2 = 1.24	0.5138
Arachidonic acid	14 ± 1.72	12.3 ± 1	12.9 ± 2	F_2 = 1.166	0.5138
EPA	0.514 ± 0.195	0.738 ± 0.033	0.75 ± 0.052	F_2 = 3.419	0.1633
DHA	3.83 ± 0.243	4.2 ± 0.395	5.14 ± 0.262***	F_2 = 25.39	0.00007

325 **Table 2:** Fatty acid profile in serum of mice treated with different formulations of yogurt. Results
326 are expressed as the percentage (%) of total fatty acids content. Data are expressed as mean ±
327 SD, n =4-5/group. # 0.05 < p < 0.10; *p < 0.05; **p < 0.01; ***p < 0.001
328

329 *Adult Hippocampal Neurogenesis*

330 In order to analyze whether the fatty acid formulation differently altered the process of
331 neurogenesis, $BrdU^+$ cells were quantified by immunohistochemistry in the DG of mice, both at
332 24 h or 4 weeks after BrdU injection to respectively evaluate the proliferative and survival stages
333 of the neurogenesis process. No significant changes were found in the proliferation of new cells
334 (p = 0.67) but it should be noted that inspection of individual data points (Fig. 2A) revealed
335 considerable within-group variability in all the experimental groups. Regarding survival of the
336 newborn cells, we found a tendency to an increase in the mice treated with the

337 nanoencapsulated formulation compared to control (ANOVA p = 0.0921, Post-hoc p =
338 0.0953941) (Fig. 2B) (Table 3).

339 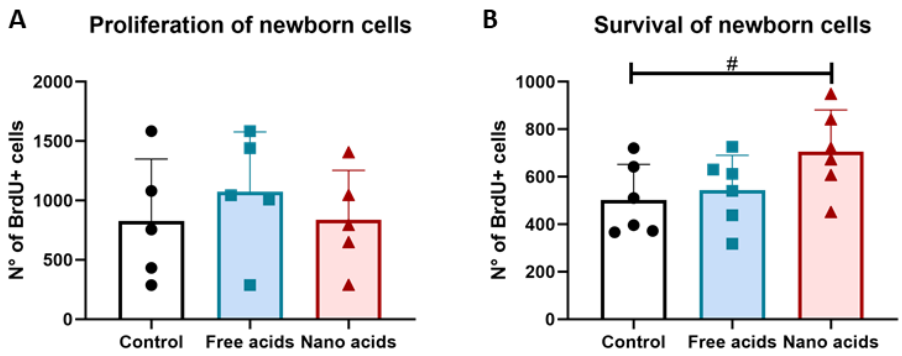

340 **Figure 2:** Adult neurogenesis process. (A) Proliferation of new cells in the dentate gyrus (DG) of
341 mice treated with fatty acids supplementation, 24 hs post injection of BrdU. (B) Survival of
342 newborn cells in the DG, 4 weeks post injection of BrdU. Data are expressed as mean ± SD, n
343 =5−6/group. # 0.05 < p < 0.10.

344

345 *RNA analysis*

346 To have an insight into mechanisms behind fatty acid fortification effects in adult neurogenesis,
347 the HC of mice were recovered after the 4 weeks of treatment and RNA expression of different
348 key molecules involved in fatty acid transport, regulation of neurogenesis, and markers of young
349 and mature neurons were analyzed.

350 As stated before, FABP5 plays a role in the uptake, transport, and metabolism of fatty acids, in
351 particular, of DHA. A tendency to a higher FABP5 expression in mice treated with the
352 nanoencapsulated yogurt formulation was detected (ANOVA p = 0.0573, Post hoc p = 0.0993)
353 (Fig. 3A) (Table 3).

354 On the other hand, BDNF has been linked to the regulation of adult hippocampal neurogenesis
355 which makes it a big candidate for being involved in the modulation of fatty acids effects in the
356 brain. Indeed, we found a significant increase in BDNF RNA after the treatment (p = 0.000766)
357 (Fig. 3B). Even though the neurotrophin expression levels were enhanced in both yogurt treated

358 groups compared to control (Free-acids p = 0.0006111; Nano-acids p = 0.0137006), expression
359 was higher after the free-fatty acids formulation (Free vs Nano p = 0.0287450) (Table 3).
360 Nestin is an intermediate filament protein that identifies neuronal progenitors and young
361 newborn neurons, while Calbindin is a calcium binding protein which serves as a marker of
362 mature, differentiated neurons. As a complementary approach to the immunohistochemistry
363 analysis, and to study the molecular profile of the tissue, we measured RNA expression of both
364 proteins. We found a significant increase in Nestin and Calbindin RNA levels after both fatty acid
365 supplementation treatments (ANOVA Nes p = 0.000271, Calb p = 0.000575). For Nestin, the free-
366 fatty acid formulation showed a higher expression (p = 0.0067782) (Fig. 3C) than the
367 nanoencapsulated acids formulation, whereas Calbindin levels were more enhanced in the
368 nanoencapsulated group (p = 0.0097060) (Fig. 3D) (Table 3). The increased expression of both
369 neuronal markers are in line with the proneurogenic effect of EPA-DHA chronic administration
370 revealed by immunohistochemistry.

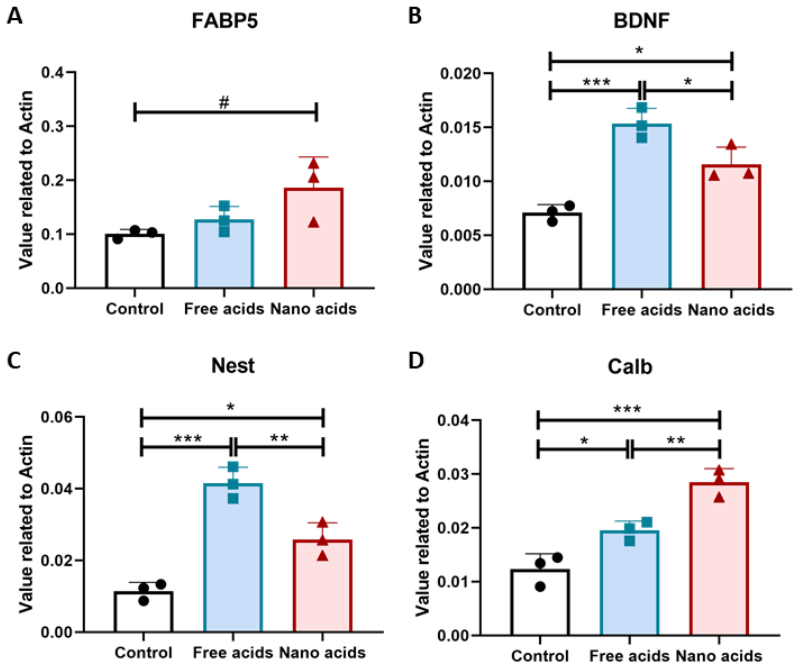

371

372 **Figure 3:** RTqPCRs. RNA was extracted from the HC of mice from the different groups to analyze
373 the transcription levels of (A) FABP5, (B) BDNF, (C) Nestin and (D) Calbindin. Data are expressed
374 as mean ± SD, n =3/group. # 0.05 < p < 0.10; *p < 0.05; **p < 0.01; ***p < 0.001

375 *BDNF Pathway*

376 To deepen the understanding of the changes produced in the BDNF pathway, which has a very
377 complex regulation, protein-expression of both BDNF isoforms and their receptors was analyzed
378 in the HC of yogurt-treated mice. Regarding the survival pathway, a significant increase was
379 observed in mBDNF levels (ANOVA p = 0.000191) only in the animals treated with the
380 nanoencapsulated yogurt formulation compared to controls (p = 0.0006301) (Fig. 4A, F),
381 whereas changes in the TrkB receptor between the treated groups and the control mice were
382 not significant (p = 0.4678826) (Fig. 4B, E) (Table 3). On the other hand, for the apoptotic
383 pathway, no significant changes were found for proBDNF (p = 0.2076) though inspection of
384 individual data points revealed considerable within-group variability in the free fatty acids group
385 (Fig. 4C, F). In addition, a tendency towards a decrease in the p75 receptor was observed in mice
386 treated with the free- fatty acid yogurt (ANOVA p = 0.0568, Ctrl vs Free p = 0.0969230) (Fig. 4D,
387 F) (Table 3), which would mean less activation of the cell death mechanisms. Results show that
388 the nanoencapsulated formulation promotes the modulation of the neurotrophin towards the
389 survival pathway, which is in accordance to the previous outcomes.

390

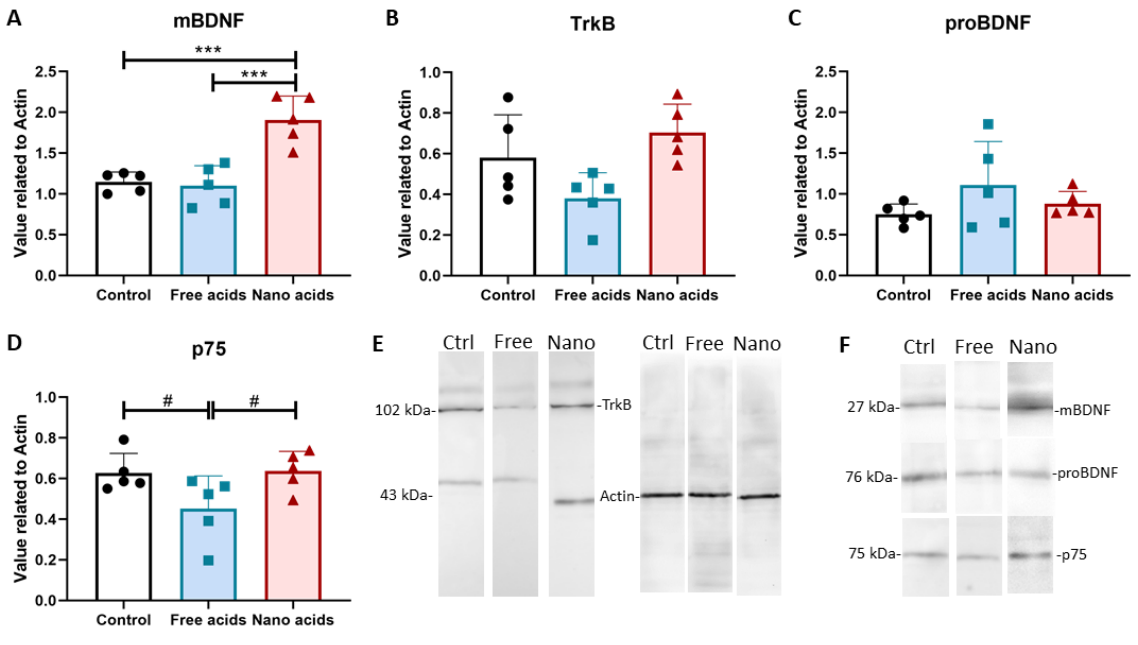

391

392 **Figure 4:** Protein expression of molecules from the BDNF signaling pathway determined by
393 Western Blot and representative membranes. (A)mBDNF. (B)TrkB. (C)proBDNF. (D)p75 for
394 yogurt treated mice after 4 weeks. (E–F) Representative membranes showing signals for TrkB,
395 mBDNF, pro-BDNF, and p75 in Control and fatty acids-treated mice. Data are expressed as mean
396 ± SD, n =5−6/group. # 0.05 < p < 0.10; *p < 0.05; **p < 0.01; ***p < 0.001.
397

Paradigm of assay	Parameter measured	Statistical test	Comparison	Statistics	P value	Figure
Body weight	Body weight	Two-way repeated measures ANOVA	Treatment	$F_{2,48}$ = 2.01	0.145	
			Week	$F_{3.12,149.77}$ = 620.92	<.001	
			Treat:Week	$F_{6.24,149.77}$ = 2.38	0.03	
Fatty acids profile	% of total Omega 3	One way ANOVA	Treatment	F_2 = 21.43	0.00016	**1A**
Fatty acids profile	% of DHA	One way ANOVA	Treatment	F_2 = 25.39	0.00007	**1B**
Fatty acids profile	% of DHA	Tukey post-test	Ctrl - Free		0.19728	
			Ctrl - Nano		0.00007	
			Free - Nano		0.00175	
Fatty acids profile	% of EPA	One way ANOVA	Treatment	F_2 = 3.419	0.1633	**1C**
Fatty acids profile	Omega6/Omega 3 ratio	One way ANOVA	Treatment	F_2 = 11.564	0.01103	**1D**
Fatty acids profile	Omega6/Omega 3 ratio	Tukey post-test	Ctrl - Free		0.214	
			Ctrl - Nano		0.019	

			Free - Nano		0.097	
Proliferation of new cells	N° of BrdU+ cells	One way ANOVA	Treatment	$F_2 = 0.414$	0.67	**2A**
Survival of newborn cells	N° of BrdU+ cells	One way ANOVA	Treatment	$F_2 = 2.807$	0.0921	**2B**
Survival of newborn cells	N° of BrdU+ cells	Tukey post-test	Ctrl - Free		0.88569	
			Ctrl - Nano		0.09539	
			Free - Nano		0.21169	
qRT-PCR	Fabp5 signal relative to actin	One way ANOVA	Treatment	$F_2 = 4.781$	0.0573	**3A**
qRT-PCR	Fabp5 signal relative to actin	Tukey post-test	Ctrl - Free		0.2399	
			Ctrl - Nano		0.0993	
			Free - Nano		0.2932	
qRT-PCR	BDNF signal relative to actin	One way ANOVA	Treatment	$F_2 = 29.79$	0.00077	**3B**
qRT-PCR	BDNF signal relative to actin	Tukey post-test	Ctrl - Free		0.00061	
			Ctrl - Nano		0.0137	
			Free - Nano		0.02874	
qRT-PCR	Nestin signal relative to actin	One way ANOVA	Treatment	$F_2 = 43.37$	0.00027	**3C**
qRT-PCR	Nestin signal relative to actin	Tukey post-test	Ctrl - Free		0.00021	
			Ctrl - Nano		0.01023	
			Free - Nano		0.00678	
qRT-PCR	Calbindin signal relative to actin	One way ANOVA	Treatment	$F_2 = 33.09$	0.00057	**3D**

qRT-PCR	Calbindin signal relative to actin	Tukey post-test	Ctrl - Free		0.02599	
			Ctrl - Nano		0.00046	
			Free - Nano		0.00971	
Western blot	mBDNF signal relative to actin	One way ANOVA	Treatment	$F_2 = 19$	0.00019	**4A**
Western blot	mBDNF signal relative to actin	Tukey post-test	Ctrl - Free		0.94531	
			Ctrl - Nano		0.00063	
			Free - Nano		0.00037	
Western blot	TrkB signal relative to actin	One way ANOVA	Treatment	$F_2 = 5.04$	0.0258	**4B**
Western blot	TrkB signal relative to actin	Tukey post-test	Ctrl - Free		0.17166	
			Ctrl - Nano		0.46788	
			Free - Nano		0.02127	
Western blot	proBDNF signal relative to actin	One way ANOVA	Treatment	$F_2 = 1.797$	0.2076	**4C**
Western blot	P75 signal relative to actin	One way ANOVA	Treatment	$F_2 = 3.678$	0.0568	**4D**
Western blot	P75 signal relative to actin	Tukey post-test	Ctrl - Free		0.09692	
			Ctrl - Nano		0.99148	
			Free - Nano		0.07893	

Table 3: P values and statistical information of all procedures performed.

399 **Discussion**

400 The results presented herein demonstrate that chronic administration of nanoencapsulated
401 PUFAs to adult mice increases the bioavailability of DHA that, in turns, may promote the survival
402 of the newborn neurons in the HC by enhancing the pro-neurogenic elements of the BDNF
403 pathway.

404 Although there are controversies regarding establishing a recommended dietary intake range
405 for the omega-6/omega-3 ratio (18–21), Zhang et al. (2024), in a UK Biobank large population
406 cohort study, revealed a strong association between the plasma omega-6/omega-3 PUFA ratio
407 and the risk of all-cause mortality, cancer, and cardiovascular disease (22). This supports dietary
408 interventions to increase omega-3 fatty acid levels and maintain a lower omega-6 to omega-3
409 fatty acid ratio as part of a healthy lifestyle.

410 In *Wistar* rats fed for 10 days a normocaloric but fat-unbalanced diet rich in saturated fats from
411 butter, supplementation with fish oil (EPA + DHA) or chia oil (ALA) increased circulating levels of
412 EPA and DHA compared to the non-supplemented group. These results indicate that the lipid
413 composition of food rapidly influences the serum fatty acid profile even in a diet rich in saturated
414 fats (14). Similarly, in the present rodent model, although PUFAs quantities ingested by different
415 animals may have varied depending on the amount of cube ingested, EPA showed a trend
416 toward higher serum concentrations in the supplemented groups, and the nanoencapsulated
417 yogurt formulation produced a significant increase in serum DHA levels. Consequently, the
418 group consuming the nanoencapsulated omega-3 yogurt exhibited a higher total n-3 fatty acid
419 content and a lower n-6/n-3 ratio, relative to the other groups (total n-3) and to the control
420 group (n-6/n-3 ratio). Indeed, in vitro studies have already demonstrated increased digestibility
421 and bioaccessibility of n-3 PUFAs when administered in nanoemulsions (7,23). Our finding
422 suggests that nanoencapsulation may protect DHA from degradation during storage and
423 digestion, thereby enhancing its stability and facilitating intestinal absorption, as reflected by
424 increased serum DHA levels. Nanoencapsulation systems might protect PUFAs from gastric

425 degradation and optimize intestinal micellization, significantly increasing their concentration (7).
426 The increased serum omega-3 levels in murine models stem from a tripartite synergy between
427 the PUFAs, the soy lecithin nanoliposomes, and the yogurt matrix. In the acidic environment
428 (pH≈4.5), nanoliposomes provide a robust physical barrier against oxidative and proton-induced
429 degradation (24). This is reinforced by a "protein-lipid corona", formed via hydrophobic and
430 electrostatic adsorption of caseins and whey proteins, which ensures steric stabilization and
431 prevents coalescence during storage and gastric transit (25). In the gastrointestinal tract, these
432 phosphatidylcholine-rich vesicles function as high-efficiency delivery vehicles. Unlike bulk oils,
433 they facilitate rapid micellization, effectively bridging the unstirred water layer to deliver
434 concentrated PUFAs to the enterocyte apical membrane (26,27). At the cellular level, soy
435 phospholipids upregulate FABP, optimizing intracellular trafficking (28). Furthermore, lecithin
436 provides essential precursors for chylomicron assembly, enhancing fatty acid re-esterification
437 and accelerating lymphatic exocytosis. Consequently, this integrated mechanism—from the
438 protective dairy-protein corona to facilitated transport—underpins the superior systemic
439 bioavailability observed (29).
440 Positive correlations between plasma and brain levels of DHA were already described (30,31).
441 Therefore, we could assume that the observed higher plasmatic levels of PUFAs may have a
442 correlate in the brain of treated mice. In the present study, the FABP-5, a key regulator of DHA
443 uptake in the brain, showed a trend to increase only in the group that received the
444 nanoencapsulated PUFAs. As this group showed the higher plasmatic levels of DHA, this result
445 could altogether show a better bioavailability and distribution of Omega-3 fatty acids under the
446 new formulation. In an elegant series of studies, Pan et al. demonstrated up-regulated
447 expression of brain microvascular FABP5 protein associated with increased brain DHA levels in
448 adult mice fed with a DHA-enriched diet for 21 days (32). Later they reported that mice knock-
449 out for the Fabp5 gene exhibited impaired performances in memory tasks, associated with a
450 reduction in endogenous brain DHA levels (33). These results, together with ours support the

451 hypothesis that increased plasmatic DHA promotes the expression of FABP-5 in the brain,
452 facilitating in turn the increase of DHA levels in the brain.
453 DHA has been inversely associated with cognitive decline in clinics (34). Indeed, populations with
454 a high consumption of fatty fish or fatty acid supplements display lower incidence of
455 neurodegenerative diseases compared to those consuming diets poor in these nutrients (35).
456 The process of neurogenesis offers a promising avenue in the search for therapies for aging and
457 neurodegenerative diseases, either by replacing lost neurons or by enhancing brain plasticity.
458 The generation of newborn neurons is well characterized in the adult hippocampus, particularly
459 in the DG, where several factors like neurotrophines, have been shown to facilitate the
460 proliferation and/or survival of newborn neurons (see rev in (36). We were not able to see
461 changes in the proliferation rate of DG neurons in adult mice receiving PUFAs, but mice treated
462 with the nanoencapsulated n-3 Omega fatty acids displayed a trend to an increase in the survival
463 of 4-week old neurons, compared with the control group. The enlarged neurogenesis was
464 accompanied by a significant increase of immature and mature markers of neuronal
465 differentiation like Nestin and Calbindin, respectively. Expression of both markers was also
466 enhanced in mice receiving the free acids, revealing that, globally, the n-3 omega fatty acids
467 appear to act at different stages of the neurogenic process, i.e, differentiation, and survival of
468 newborn neurons. Increased neuron survival has been already shown in a model of strong deficit
469 of PUFA where rats fed a fish-oil deficient diet for three generations were then, supplemented
470 with DHA for 7 weeks (37). Another report from rats fed a DHA and EPA-enriched diet during 4
471 weeks revealed an increase in hippocampal levels of the BDNF as measured by ELISA (10). Similar
472 results were observed for BDNF mRNA and protein levels in a transgenic mice model of
473 Alzheimer's disease after 2 months of a DHA-enriched diet (11) and in C57BL/6 mice chronically
474 supplemented with lysophosphatidylcholine-DHA or -EPA (38,39). Our results shed light on
475 these reports describing plastic effects of PUFAs in rodents, as we were able to go deep in the
476 analysis of the BDNF biological pathway. In this study, increased levels of total BDNF mRNA were

477 detected in both groups of mice that received the n-3 omega fatty acids compared to the control
478 groups. However, when the level of proteins were analyzed, mice receiving the free fatty acids
479 showed a sort of activation of the BDNF pro-apoptotic cascade, with a tendency towards higher
480 levels of the p-75 receptor and something similar for pro-BDNF compared to the other
481 experimental groups. In this line, a previous study in a mice model of Alzheimer disease found
482 that the administration of a DHA/EPA-enriched diet for 2 months decreased the expression of
483 pro-apoptosis factors like Bcl2, Caspase 3, and Caspase 9 (11). On the contrary, the
484 proneurogenic elements of this biological pathway, like mBDNF and its receptor TrkB, were
485 significantly increased after chronic administration of nanoencapsulated PUFAs, in synthon with
486 the increased survival of the newborn neurons detected in the DG.
487

488 **Conclusions**

489 In this work, nanoencapsulated PUFAs orally administrated to male mice for 4 or 8 weeks
490 showed better bioavailability when compared to administration of free acids, and this
491 potentially due to an increase of the specific transporter, the FABP-5 particularly in the HC.
492 Furthermore, the nanoformulation enhanced the survival of the DG newborn neurons, possibly
493 in response to an improved proneurogenic balance of BDNF actions. These positive effects can
494 be key to facilitate memory processes and also, to prevent cognitive decline that can occur at
495 advanced ages.
496

497 **References**

498 1. McNamara RK, Carlson SE. Role of omega-3 fatty acids in brain development and
499 function: Potential implications for the pathogenesis and prevention of
500 psychopathology. Prostaglandins Leukot Essent Fatty Acids. 2006;75:329–349. doi:
501 10.1016/j.plefa.2006.07.010. Cited in PMID: 16949263.

502 2. Rahim MA, Uzma M, Al-Asmari F, Koraqi H, Ramadan MF, Castro-Muñoz R, Zongo E. A
503 Comprehensive Review on Nutritional Traits, Extraction Methods, Oxidative Stability,
504 Encapsulation Technologies, Food Applications and Health Benefits of Omega Fatty
505 Acids. Food Sci Nutr. 2025;13. doi: 10.1002/fsn3.71008.

506 3. Mitchell RW, On NH, Del Bigio MR, Miller DW, Hatch GM. Fatty acid transport protein
507 expression in human brain and potential role in fatty acid transport across human brain
508 microvessel endothelial cells. J Neurochem. 2011;117:735–746. doi: 10.1111/j.1471-
509 4159.2011.07245.x. Cited in PMID: 21395585.

510 4. Iwao T, Takata F, Matsumoto J, Aridome H, Yasunaga M, Yokoya M, Kataoka Y, Dohgu S.
511 Aging decreases docosahexaenoic acid transport across the blood-brain barrier in
512 C57BL/6J mice. PLoS One. 2023;18. doi: 10.1371/journal.pone.0281946. Cited in PMID:
513 36795730.

514 5. Clemente-Suárez VJ, Beltrán-Velasco AI, Redondo-Flórez L, Martín-Rodríguez A,
515 Tornero-Aguilera JF. Global Impacts of Western Diet and Its Effects on Metabolism and
516 Health: A Narrative Review. Nutrients. 2023;15. doi: 10.3390/nu15122749. Cited in
517 PMID: 37375654.

518 6. Inapurapu SP, Ibrahim A, Kona SR, Pawar SC, Bodiga S, Bodiga VL. Development and
519 characterization of ω-3 fatty acid nanoemulsions with improved physicochemical
520 stability and bioaccessibility. Colloids Surf A Physicochem Eng Asp. 2020;606. doi:
521 10.1016/j.colsurfa.2020.125515.

522 7. Yang J, Ciftci ON. In vitro bioaccessibility of fish oil-loaded hollow solid lipid micro- A nd
523 nanoparticles. Food Funct. 2020;11:8637–8647. doi: 10.1039/d0fo01591a. Cited in
524 PMID: 32936172.

525 8. Kempermann G, Song H, Gage FH. Neurogenesis in the adult hippocampus. Cold Spring
526 Harb Perspect Biol. 2015;7:a018812. doi: 10.1101/cshperspect.a018812. Cited in PMID:
527 26330519.

528 9. Foltran RB, Diaz SL. BDNF isoforms: a round trip ticket between neurogenesis and
529 serotonin? J Neurochem. 2016;138:204–221. doi: 10.1111/jnc.13658.

530 10. Wu A, Ying Z, Gomez-Pinilla F. Dietary Omega-3 Fatty Acids Normalize BDNF Levels,
531 Reduce Oxidative Damage, and Counteract Learning Disability after Traumatic Brain
532 Injury in Rats. J Neurotrauma. 2004;21.

533 11. Che H, Zhou M, Zhang T, Zhang L, Ding L, Yanagita T, Xu J, Xue C, Wang Y. Comparative
534 study of the effects of phosphatidylcholine rich in DHA and EPA on Alzheimer's disease
535 and the possible mechanisms in CHO-APP/PS1 cells and SAMP8 mice. Food Funct.
536 2018;9:643–654. doi: 10.1039/c7fo01342f. Cited in PMID: 29292421.

537 12. FAO, WHO. Report of the Joint FAO/WHO Expert Consultation on the Risks and Benefits
538 of Fish Consumption. Rome; 2011.

539 13. Foltran RB, Stefani KM, Hocht C, Diaz SL. Neurochemical, behavioral, and neurogenic
540 validation of a hyposerotonergic animal model by voluntary oral consumption of PCPA.
541 ACS Chem Neurosci. 2020; doi: 10.1021/acschemneuro.9b00687.

542 14. Fernandez I, Giacomino MS, Condori AI, Godoy MF, Pellegrino N, Slobodianik N, Feliu
543 MS. Effect of n-3 fatty acids supplementation on serum lipid profile of rats. Revista
544 Chilena de Nutricion. 2021;48:170–178. doi: 10.4067/S0717-75182021000200170.

545 15. Schneider CA, Rasband WS, Eliceiri KW. NIH Image to ImageJ: 25 years of image
546 analysis. Nat Methods [Internet]. 2012;9:671–675. Cited in PMID: 22930834.

547 16. Bustin SA, Benes V, Garson JA, Hellemans J, Huggett J, Kubista M, Mueller R, Nolan T,
548 Pfaffl MW, Shipley GL, et al. The MIQE guidelines: Minimum information for publication
549 of quantitative real-time PCR experiments. Clin Chem. 2009;55:611–622. doi:
550 10.1373/clinchem.2008.112797. Cited in PMID: 19246619.

551 17. Diaz SL, Doly S, Narboux-Nême N, Fernández S, Mazot P, Banas SM, Boutourlinsky K,
552 Moutkine I, Belmer A, Roumier A, et al. 5-HT2B receptors are required for serotonin-
553 selective antidepressant actions. Mol Psychiatry. 2012;17:154. doi:
554 10.1038/mp.2011.159. Cited in PMID: 22158014.

555 18. Food and Agriculture Organization [FAO]. Fats and fatty acids in human nutrition:
556 report of an expert consultation. FAO Food Nutr Pap. 2010;91:1–166.

557 19. EFSA Panel on Dietetic Products N and A (NDA). Scientific Opinion on the Tolerable
558 Upper Intake Level of eicosapentaenoic acid (EPA), docosahexaenoic acid (DHA) and
559 docosapentaenoic acid (DPA). EFSA Journal. 2012;10. doi: 10.2903/j.efsa.2012.2815.

560 20. Simopoulos AP. The importance of the omega-6/omega-3 fatty acid ratio in
561 cardiovascular disease and other chronic diseases. Exp Biol Med. 2008;233:674–688.
562 doi: 10.3181/0711-MR-311. Cited in PMID: 18408140.

563 21. Djuricic I, Calder PC. Beneficial outcomes of omega-6 and omega-3 polyunsaturated
564 fatty acids on human health: An update for 2021. Nutrients. 2021;13. doi:
565 10.3390/nu13072421. Cited in PMID: 34371930.

566 22. Zhang Y, Sun Y, Yu Q, Song S, Thomas Brenna J, Shen Y, Ye K. Higher ratio of plasma
567 omega-6/omega-3 fatty acids is associated with greater risk of all-cause, cancer, and
568 cardiovascular mortality: A population-based cohort study in UK Biobank. Elife.
569 2023;12:90132. doi: 10.7554/eLife.

570 23. Zhou Q, Lane KE, Li W. Evaluating the Stability and Digestibility of Long-Chain Omega-3
571 Algal Oil Nanoemulsions Prepared with Lecithin and Tween 40 Emulsifiers Using an In
572 Vitro Digestion Model. Foods. 2024;13. doi: 10.3390/foods13152407.

573 24. Ghorbanzade T, Jafari SM, Akhavan S, Hadavi R. Nano-encapsulation of fish oil in nano-
574 liposomes and its application in fortification of yogurt. Food Chem. 2017;216:146–152.
575 doi: 10.1016/j.foodchem.2016.08.022. Cited in PMID: 27596403.

576 25. Taneja A, Ye A, Singh H. Effects of the milk matrix on the bioavailability of vitamins and
577 minerals. In: McLean JK, Anderson AS, editors. Food-based approaches for a healthy
578 diet. Woodhead Publishing; 2010. p. 233–256.

579 26. Kim YM, Jang GH, Seok CH, Kim BH, Bae JW, Kim BH, Yoon MS. A self-emulsifying
580 omega-3 fatty acids delivery system for enhanced gastro-intestinal absorption in rats.
581 Food Science and Biotechnology 2022 31:13 [Internet]. 2022 [cited 2026 Mar
582 11];31:1631–1638. doi: 10.1007/s10068-022-01151-7.

583 27. Ahmmed MK, Ahmmed F, Tian H, Carne A, Bekhit AED. Marine omega-3 (n-3)
584 phospholipids: A comprehensive review of their properties, sources, bioavailability, and
585 relation to brain health. Compr Rev Food Sci Food Saf. 2020;19:64–123. doi:
586 10.1111/1541-4337.12510. Cited in PMID: 33319514.

587 28. Lane KE, Li W, Smith C, Derbyshire E. The bioavailability of an omega-3-rich algal oil is
588 improved by nanoemulsion technology using yogurt as a food vehicle. Int J Food Sci
589 Technol. 2014;49:1264–1271. doi: 10.1111/ijfs.12455.

590 29. Mozafari MR, Johnson C, Hatziantoniou S, Demetzos C. Nanoliposomes and their
591 applications in food nanotechnology. J Liposome Res. 2008;18:309–327. doi:
592 10.1080/08982100802465941. Cited in PMID: 18951288.

593 30. Hashimoto M, Hossain S, Shimada T, Sugioka K, Yamasaki H, Fujii Y, Ishibashi Y, Oka JI,
594 Shido O. Docosahexaenoic acid provides protection from impairment of learning ability
595 in Alzheimer's disease model rats. J Neurochem. 2002;81:1084–1091. doi:
596 10.1046/j.1471-4159.2002.00905.x. Cited in PMID: 12065621.

597 31. Orchard TS, Gaudier-Diaz MM, Phuwamongkolwiwat-Chu P, Andridge R, Lustberg MB,
598 Bomser J, Cole RM, Belury MA, Devries AC. Low sucrose, omega-3 enriched diet has
599 region-specific effects on neuroinflammation and synaptic function markers in a mouse
600 model of doxorubicin-based chemotherapy. Nutrients. 2018;10. doi:
601 10.3390/nu10122004. Cited in PMID: 30567351.

602 32. Pan Y, Morris ER, Scanlon MJ, Marriott PJ, Porter CJH, Nicolazzo JA. Dietary
603 docosahexaenoic acid supplementation enhances expression of fatty acid-binding
604 protein 5 at the blood–brain barrier and brain docosahexaenoic acid levels. J
605 Neurochem. 2018;146:186–197. doi: 10.1111/jnc.14342. Cited in PMID: 29582413.

606 33. Pan Y, Short JL, Choy KHC, Zeng AX, Marriott PJ, Owad Y, Scanlon MJ, Porte CJH,
607 Nicolazzo JA. Fatty acid-binding protein 5 at the blood–brain barrier regulates
608 endogenous brain docosahexaenoic acid levels and cognitive function. Journal of
609 Neuroscience. 2016;36:11755–11767. doi: 10.1523/JNEUROSCI.1583-16.2016. Cited in
610 PMID: 27852782.

611 34. Mallick R, Basak S, Duttaroy AK. Docosahexaenoic acid,22:6n-3: Its roles in the structure
612 and function of the brain. International Journal of Developmental Neuroscience.
613 2019;79:21–31. doi: 10.1016/j.ijdevneu.2019.10.004. Cited in PMID: 31629800.

614 35. Kalmijn S, Van Boxtel MPJ, Ocké M, Verschuren WMM, Kromhout D, Launer LJ. Dietary
615 intake of fatty acids and fish in relation to cognitive performance at middle age.
616 Neurology. 2004;62:275–280.

617 36. Balu DT, Lucki I. Adult hippocampal neurogenesis: Regulation, functional implications,
618 and contribution to disease pathology. Neurosci Biobehav Rev. 2009;33:232–252. doi:
619 10.1016/j.neubiorev.2008.08.007. Cited in PMID: 18786562.

620 37. Kawakita E, Hashimoto M, Shido O. Docosahexaenoic acid promotes neurogenesis in
621 vitro and in vivo. Neuroscience. 2006;139:991–997. doi:
622 10.1016/j.neuroscience.2006.01.021.

623 38. Sugasini D, Thomas R, Yalagala PCR, Tai LM, Subbaiah P V. Dietary docosahexaenoic acid
624 (DHA) as lysophosphatidylcholine, but not as free acid, enriches brain DHA and
625 improves memory in adult mice. Sci Rep. 2017;7. doi: 10.1038/s41598-017-11766-0.
626 Cited in PMID: 28900242.

627 39. Yalagala PCR, Sugasini D, Dasarathi S, Pahan K, Subbaiah P V. Dietary
628 lysophosphatidylcholine-EPA enriches both EPA and DHA in the brain: Potential

treatment for depression. J Lipid Res. 2019;60:566–578. doi: 10.1194/jlr.M090464. Cited in PMID: 30530735.